



Adsorption of Zn²⁺ in wastewater by vinylamine modified weathered coal

Yajuan Cheng^a, Xinyue Ma^a, Yanxu Chi^a, Xiaoli Ma^{b,*}

^aCollege of Chemistry and Chemical Engineering, Xinjiang Normal University, Urumqi 830054, Xinjiang, China, Tel. +13369074215; email: 1749824793@qq.com (Y. Cheng), Tel. +15999152767; email: 2452578448@qq.com (X. Ma), Tel. +18199142403; email: 1141612570@qq.com (Y. Chi)

^bXinjiang Key Laboratory of Energy Storage and Photoelectrolytic Materials, Urumqi 830054, Xinjiang, China, Tel. +18299198975; email: 68186793@qq.com (X. Ma)

Received 30 September 2021; Accepted 1 June 2022

ABSTRACT

Zinc adsorption was analyzed in a Xinjiang weathered coal (XWC) matrix, modified by four vinyl amines: diethylenetriamine (DETA), and triethylenetetramine (TETA), tetraethylenepentamine (TEPA), and pentaethylenehexamine (PEHA). Four aminated coal-based adsorbents, weathered coal modified by DETA (TAWC-1), weathered coal modified by TETA (TAWC-2), weathered coal modified by TEPA (PAWC), and weathered coal modified by PEHA (HAWC), were prepared by a cross-linking reaction combined with ultrasonic vibration and were characterized by Fourier transform infrared spectroscopy, X-ray photoelectron spectroscopy, and specific surface area and pore size distribution analysis. The four adsorbents were compared by examining the influence of pH, amount of adsorbent, reaction time, and other factors on the adsorption process. The results showed that the polyethyleneimine polyamine in vinylamine was successfully grafted onto the pulverized coal surface, the specific surface area and pore volume showed a decreasing trend with an increasing number of amino groups, the optimal pH values of XWC, TAWC-1, TAWC-2, PAWC, and HAWC are 12.0, 8.0, 8.0, 8.0, and 7.0, respectively, the optimal dosages are 1.3, 0.6, 0.5, 0.5, and 0.4 g, respectively and the optimal reaction times are 70, 30, 30, 25, and 25 min, respectively. The adsorption processes of Zn²⁺ by XWC, TAWC-1, TAWC-2, PAWC, and HAWC were consistent with the pseudo-second-order kinetic model and Langmuir adsorption isotherm equation. The fitted saturated adsorption capacities of XWC, TAWC-1, TAWC-2, PAWC, and HAWC were 36.76, 109.89, 133.23, 163.93, and 192.31 mg/g, respectively, which were 3.0, 3.6, 4.6, and 5.2 higher than those before modification.

Keywords: Vinylamine; Modification; Weathered coal; Zinc adsorption in wastewater

1. Introduction

Zinc in wastewater mainly derives from industries such as electroplating and smelting [1]. High concentrations of zinc in wastewater can have adverse effects if the water is directly discharged into the environment without treatment. Studies have shown that excessive consumption of zinc in the human body can cause diseases such as copper deficiency and anemia [2] and that Zn²⁺ inhibits the expression

of p53 in cancer cells [3], leading to a delay in the detection of cancer. Therefore, the effective treatment of zinc in wastewater is extremely important for public health and environmental safety. At present, the methods of treating zinc-containing wastewater include chemical precipitation [4], flotation [5], ion exchange [6], electrochemistry [7], and adsorption [8]. Among these methods, chemical precipitation and flotation involve a complex procedure whereby a pH change is induced by adding sodium hydroxide,

* Corresponding author.

and ion exchange [9,10], and electrochemistry involves high operating costs and complex processes. The adsorption method, however, is simple and does not introduce secondary pollution; therefore, it is considered one of the most effective sewage treatment technologies [11].

At present, common adsorbents include activated carbon [12,13], zeolite [14,15], kaolin [16,17], and bentonite [18,19], carbon nanotubes [20,21]. Although they have their own advantages, they are typically expensive and have the problem of low adsorption capacity. For the treatment of industrial zinc-containing wastewater, a more economical and effective adsorbent should be found. Weathered coal has a wide range of sources and low prices and has some adsorption capacity [22,23]. It is often used to modify alkaline soil [24] or to improve the storage stability of asphalt [25,26]. Through modification, its adsorption capacity can be improved, and can therefore be used to treat industrial zinc-containing wastewater. As a low-cost adsorbent, it has great development value.

In this study, a simulation of zinc-containing wastewater adsorption was analyzed in a Xinjiang weathered coal (XWC) matrix, modified by four vinylamines: diethylenetriamine (DETA), triethylenetetramine (TETA), tetraethylenepentamine (TEPA), and pentaethylenehexamine (PEHA). Four aminated coal-based adsorbents, triamine weathered coal (TAWC-1), tetramine weathered coal (TAWC-2), pentamidine weathered coal (PAWC), and hexamine weathered coal (HAWC), were prepared by a cross-linking reaction combined with ultrasonic vibration. They were characterized by scanning electron microscopy (SEM), infrared (IR), X-ray photoelectron spectroscopy (XPS), and specific surface area and pore size distribution analysis. The four adsorbents were compared by examining the influence of pH, amount of adsorbent, reaction time, and other factors on the adsorption process, the innovation of this paper lies in the modification of weathered coal with DETA, TETA, TEPA, and PEHA, the influence of the number of amino groups on the modification effect is systematically compared for the first time, which provides a preliminary basis for the further modification of ethylene amine.

2. Experimental section

2.1. Reagents and major equipment

The materials used in this study were sodium hydroxide (AR grade), sulfuric acid (AR grade), zinc sulfate (AR grade), diethylenetriamine (DETA, AR grade), triethylenetetramine (TETA, AR grade), tetraethylenepentamine (TEPA, AR grade), and pentaethylenehexamine (PEHA, AR grade). Deionized water (electrical resistivity > 18.2 M Ω ·cm) was used as the test water.

For the analysis, we used a JY92-2D ultrasonic cell disruptor (Ningbo Scientz Biotechnology Co. Ltd.), a Z-2000 atomic adsorption spectrometer (HITACHI, Japan), a SU-8000 high-resolution field emission scanning electron microscope (HITACHI, Japan), an ASIQM0002-6 specific surface area and pore size distribution tester (Quantachrome Instruments, US), a TENSOR27 infrared spectrometer (Bruker Optics), and an ESCALAB 250Xi X-ray photoelectron spectrometer (Thermo Fisher Scientific, US).

2.2. Preparation of adsorbents

5 g of XWC was weighed and placed in a 100 mL beaker, which was sealed with weighing paper and placed in an oven for thermostatic activation at 80°C for 24 h. After cooling to room temperature, 40 mL of deionized water was added, followed by 3 mL diethylenetriamine, 2.5 mL triethylenetetramine, and 2.5 mL tetraethylenepentamine, and 2 mL pentaethylenehexamine, respectively, and the solution was stirred to ensure thorough mixing. The beaker was then placed in an ultrasonic cell disruptor and, after adjusting the ultrasonic power, the solution oscillated for a certain period of time. After the reaction, the product was centrifuged, and the supernatant was discarded. The solid phase was repeatedly washed with deionized water until the supernatant was neutral. After drying, it was ground to less than 200 mesh (0.075 mm) to obtain four aminated coal-based adsorbents, which were placed into sealed bags for later use.

2.3. Adsorbent material characterization

2.3.1. SEM test

The dried samples were sprayed with gold, and the shape and morphology of their particles were observed with the scanning electron microscope (SEM) at an accelerating voltage of 15 kV.

2.3.2. Aperture distribution test

The samples were treated under a vacuum at 200°C for 12 h before the test. The N₂ adsorption–desorption experiment was performed at –196°C (using liquid nitrogen), and the specific surface areas of the samples were calculated by the BET (Brunauer–Emmet–Teller) model. The BJH (Barrett–Joyner–Halenda) equivalent cylinder model was used to calculate the pore size distribution and the total pore volume was determined by N₂ adsorption at a relative pressure of 0.995.

2.3.3. Fourier transform infrared spectroscopy test

The samples and KBr were taken, mixed evenly, tableted, and placed in a Fourier transform infrared spectroscopy to be tested in a wavenumber range of 4,000–400 cm⁻¹.

2.3.4. XPS test

AlK α radiation was used as the X-ray source, and a C_{1s} binding energy at 285.0 eV was used for calibration. The samples were then subjected to photoelectron spectroscopy.

2.4. Adsorption test

The adsorption test was carried out by the batch process method to study the effects of adsorbent dosage, system pH, reaction time, and initial $\rho(\text{Zn}^{2+})$ of the solution on the adsorption process. The specific process was as follows: 50 mL of simulated wastewater at a certain concentration was added to a 100 mL beaker. A certain amount of adsorbent was then weighed and taken. The pH of the system

was adjusted with 1 mol/L NaOH and 1 mol/L H₂SO₄ solution. After being placed on a magnetic stirrer and stirred for a period of time, the solution was transferred to a centrifuge tube for centrifugation for 10 min, a certain volume of supernatant was taken, and the $\rho(\text{Zn}^{2+})$ was determined by flame atomic absorption spectrometry to calculate the removal rate (R): Eq. (1) and adsorption quantity (Q_e): Eq. (2).

$$R = \frac{(C_0 - C_e)}{C_0} \times 100\% \quad (1)$$

$$Q_e = \frac{[(C_0 - C_e)V]}{m} \quad (2)$$

where C_0 (mg/L) and C_e (mg/L) are $\rho(\text{Zn}^{2+})$ values of the solution at initiation and equilibrium respectively, R (%) is the removal rate of Zn^{2+} , Q_e (mg/g) is the adsorption

capacity at equilibrium, V (mL) is the solution volume, and m (g) is the adsorbent dosage.

3. Results and discussion

3.1. Surface characterization

3.1.1. SEM analysis

SEM images of weathered coal before and after modification are shown in Fig. 1. Naturally weathered coal (XWC) has an irregular layered structure with a rough surface and large particles, triamine weathered coal (TAWC-1) shows clear rod-like structures, tetramine weathered coal (TAWC-2) has coexisting rod-like and layered structures, pentamidine weathered coal (PAWC) exhibits flaky structures with clear separation of layers, and hexamine weathered coal (HAWC) has irregular layered structures with closely linked layers. This shows that ultrasonic oscillation removes the impurities in the pores of coal powder and that vinylamine is adhesive. According to the changes observed

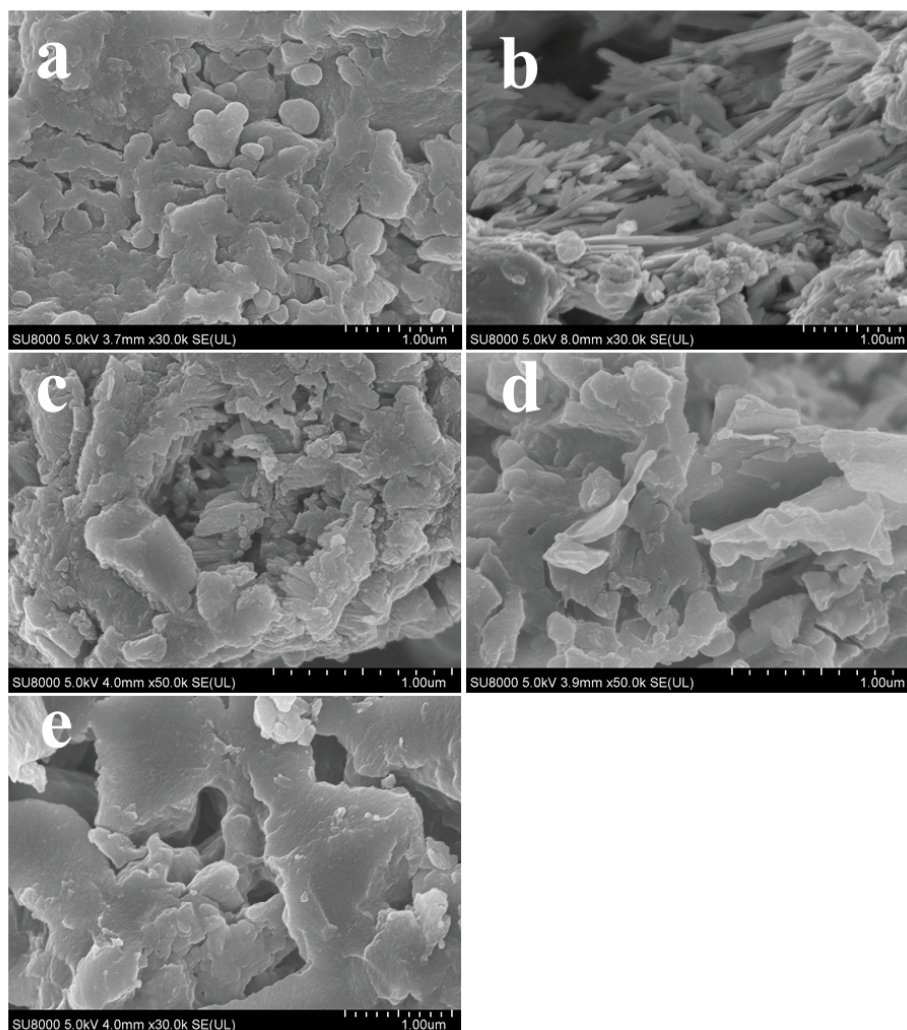


Fig. 1. SEM spectrogram for weathered coal: (a) XWC, (b) TAWC-1, (c) TAWC-2, (d) PAWC, and (e) HAWC.

from panels b to e, the greater the number of amino groups, the stronger the adhesiveness of vinylamine; therefore, the smaller the specific surface area.

3.1.2. BET analysis

Table 1 shows the pore size distribution data of weathered coal before and after modification. Fig. 2 shows the N_2 adsorption–desorption isotherm curves of weathered coal before and after modification. It is clear that all weathered coal has a pore size of approximately 3.83 nm, which belongs to the category of mesoporous materials (Table 1). With an increasing number of amino groups, the specific surface area of the aminated coal-based adsorbent decreases from 3.729 to 1.624 m^2/g , and the pore volume decreases from 0.006 to 0.003 cm^3/g . This result is consistent with the SEM analysis and shows that the active groups in vinylamine entered the pores and adhered to the surface of pulverized coal simultaneously, resulting in the decrease of specific surface area and pore volume.

3.1.3. Fourier transform infrared spectroscopy analysis

Fig. 3 shows the IR spectra of weathered coal before and after modification. XWC shows adsorption peaks at 3,428;

1,716; 1,586; 1,354; 1,244 and 790 cm^{-1} . Among them, the broad peaks at 3,428 cm^{-1} come from the stretching vibration of $-OH$ and the stretching vibration of $-NH$ [27]. The spike at 1,716 cm^{-1} relates to the stretching vibration of $-C=O$, the spike at 1,586 cm^{-1} is from the bending vibration of $-NH$, the spike at 1,354 cm^{-1} is assigned to the symmetrical stretching vibration of $-CH$, the spike at 1,244 cm^{-1} comes from the stretching vibration of $-OH$, and the spike at 790 cm^{-1} is assigned to the bending vibration of $-CH$. Compared with XWC, the peaks at 1,716 and 1,244 cm^{-1} disappear in the modified amine-based weathered coal, and the peak intensity at 3,428 cm^{-1} is reduced. With an increasing number of amino groups, the magnitude of the blue shift of the $-NH$ peak at 1,586 cm^{-1} increases gradually, and the $-OH$ peak at 1,244 cm^{-1} disappears gradually after the redshift. This indicates that the polyethylene polyamine in vinylamine chemically reacts with $-C=O$ and $-OH$ on the surface of the weathered coal, resulting in the masking of these two functional groups.

3.1.4. XPS analysis

Table 2 shows the element contents of the weathered coal before and after modification and Fig. 4 shows the XPS spectrum of weathered coal before and after modification. Both before and after modification, the weathered coal exhibits

Table 1
Surface characterization of XWC, TAWC-1, TAWC-2, PAWC, and HAWC coal

Adsorbent	Specific surface area (m^2/g)	Pore volume (cm^3/g)	Pore size (nm)
XWC	6.875	0.010	3.829
TAWC-1	3.729	0.006	3.832
TAWC-2	3.440	0.005	3.829
PAWC	1.709	0.004	3.838
HAWC	1.624	0.003	3.830

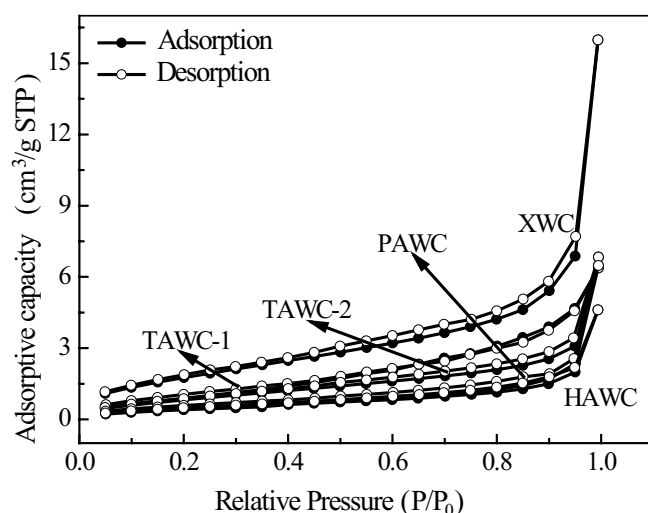


Fig. 2. Nitrogen adsorption/desorption isotherms of XWC, TAWC-1, TAWC-2, PAWC, and HAWC.

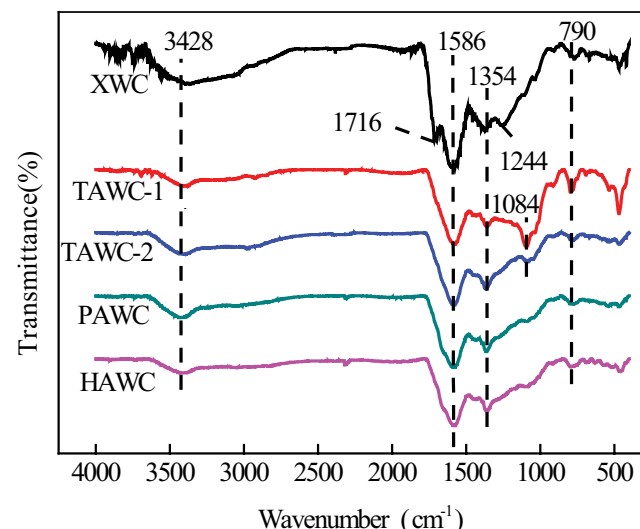


Fig. 3. IR spectrogram for XWC, TAWC-1, TAWC-2, PAWC, and HAWC coals.

Table 2
Elemental composition of XWC, TAWC-1, TAWC-2, PAWC, and HAWC coal

Atomic %	C _{1s}	O _{1s}	N _{1s}	S _{2p1}	Si _{2p}
XWC	72.64	22.90	2.16	0.5	1.80
TAWC-1	71.82	21.17	6.31	0.44	0.26
TAWC-2	70.87	20.95	7.34	0.2	0.64
PAWC	70.37	20.55	8.10	1.3	0.85
HAWC	69.57	20.04	8.38	0.48	1.50

O_{1s} , N_{1s} , C_{1s} , S_{2p1} , and Si_{2p} characteristic peaks at 531.46, 400.08, 282.74, 153.36, and 101.21 eV (Fig. 4). With increasing amino groups, the intensity of the N_{1s} peak gradually increases. The N content in the aminated coal-based adsorbent gradually increases and the C and O contents gradually decrease (Table 2), indicating that the amino groups in the vinylamine react with $-C=O$ and $-OH$ during modification, and vinylamine is successfully grafted to the surface of the pulverized coal. This result is consistent with the IR result.

3.2. Factors affecting adsorption

3.2.1. Adsorbent dosage

The effect of adsorbent dosage on Zn^{2+} removal from wastewater is shown in Fig. 5. The removal rate of Zn^{2+} by weathered coal before and after modification first increases

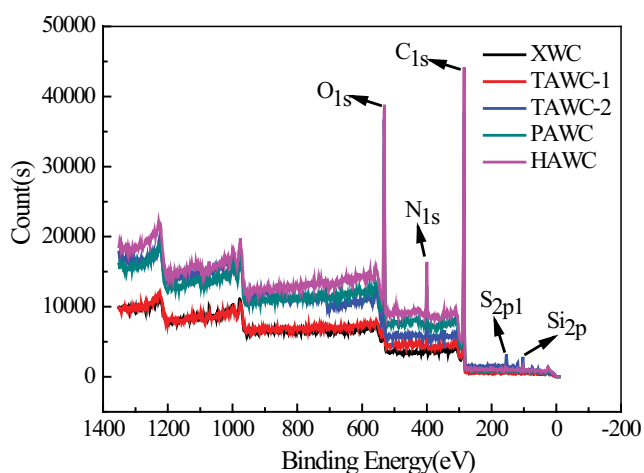


Fig. 4. XPS spectrogram for XWC, TAWC-1, TAWC-2, PAWC, and HAWC coal.

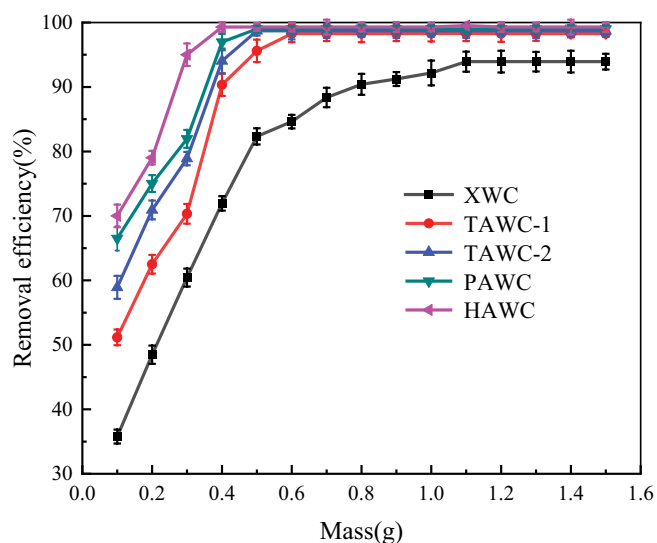


Fig. 5. Effects of sorbent dosage on Zn^{2+} removal. Adsorption temperature = 298 K; initial $\rho(Zn^{2+}) = 600$ mg/L; pH = 7.0; reaction time = 60 min.

and then stabilizes. The optimal dosages of XWC, TAWC-1, TAWC-2, PAWC, and HAWC are 1.3, 0.6, 0.5, 0.5, and 0.4 g, respectively. When $\rho(Zn^{2+})$ is constant in the wastewater, the number of adsorption sites in the solution and the removal rate increase with increasing adsorbent dosage. When the adsorbent dosage increases to a certain extent, a shielding effect forms among the periphery of adsorbent particles preventing the binding of Zn^{2+} to adsorption sites [28], and the removal rate tends to plateau.

3.2.2. System pH

Fig. 6 shows the effect of system pH on Zn^{2+} removal. XWC has a high removal rate in a pH range of 5–12 and a maximum removal rate at a pH of 12. The modified weathered coal and HAWC have high removal rates in a pH range of 4–12. The optimal pH values of XWC, TAWC-1, TAWC-2, PAWC, and HAWC are 12.0, 8.0, 8.0, 8.0, and 7.0, respectively. The effect of pH on Zn^{2+} adsorption is mainly related to the surface charge characteristics of the adsorbent. When it's in the smaller pH range, a large amount of free H^+ in the solution protonates $-NH$ on the surface of weathered coal to $-NH_2^+$ and electrostatic repulsion produced by Zn^{2+} results in a low removal rate [29]. When it's in the larger pH range, protonation no longer occurs and the Zn^{2+} floats to the surface of the adsorbent driven by the gravitational force of the charge [30]. As a result, the removal rate increases and finally becomes balanced.

3.2.3. Reaction time

Fig. 7 shows the effect of different reaction times on the adsorption effect at 25°C, 30°C, and 35°C. The influence of temperature on the adsorption process is relatively small; the maximum removal rate can be achieved at room temperature, and the removal rate increases with temperature. Therefore, all adsorption experiments were carried

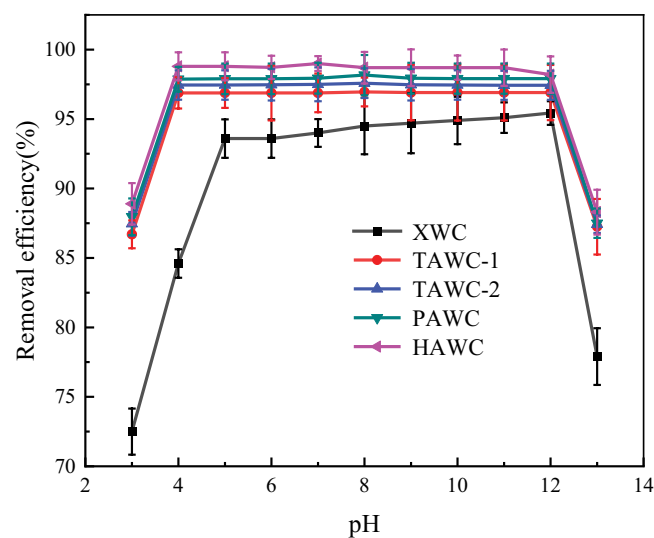


Fig. 6. Effects of pH on Zn^{2+} removal. Adsorption temperature = 298 K; initial $\rho(Zn^{2+}) = 600$ mg/L; reaction time = 60 min; $m(XWC) = 1.3$ g; $m(TAWC-1) = 0.6$ g; $m(TAWC-2) = 0.5$ g; $m(PAWC) = 0.5$ g; $m(HAWC) = 0.4$ g.

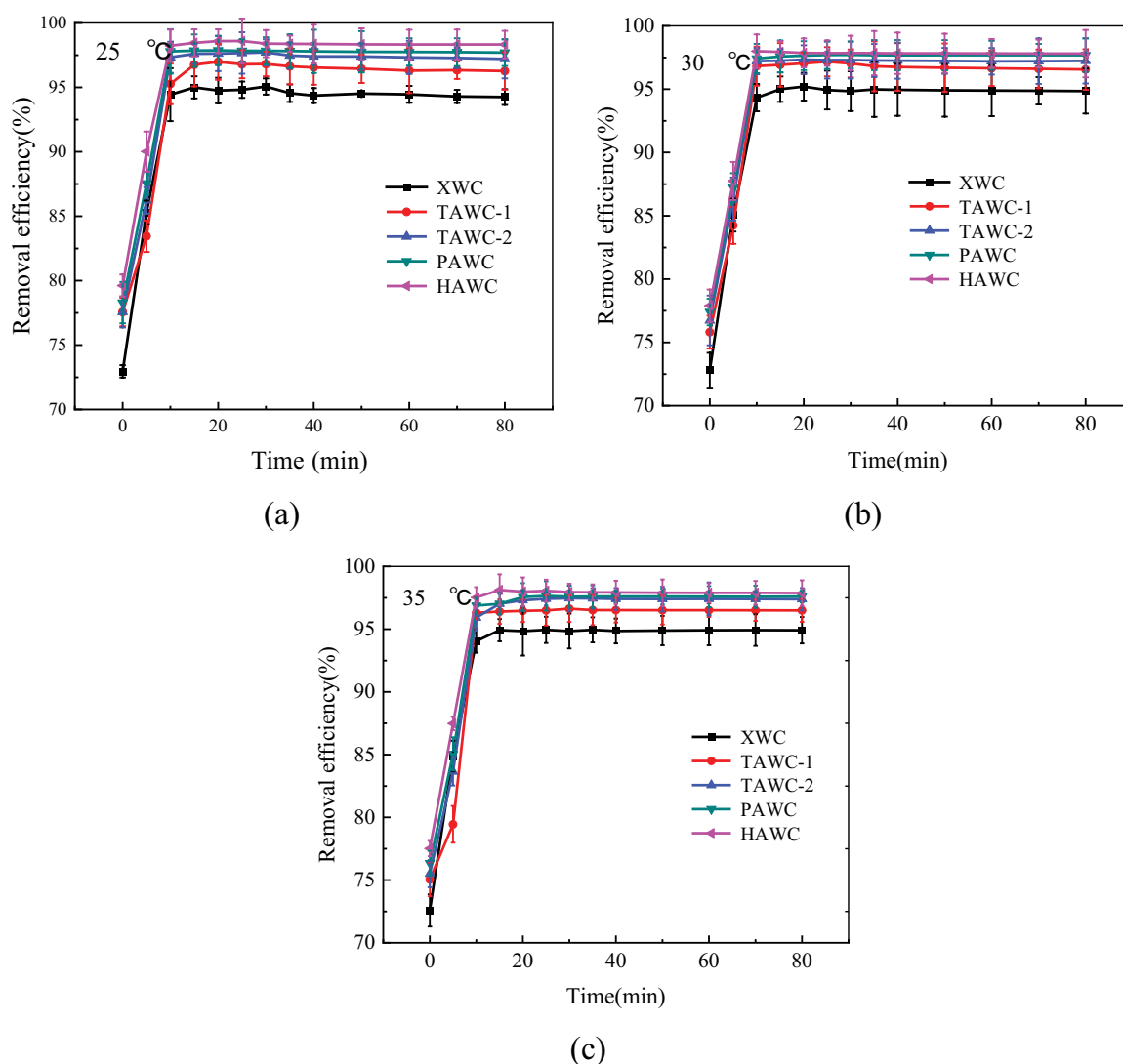


Fig. 7. Effects of contact time on Zn²⁺ removal. Initial $\rho(\text{Zn}^{2+}) = 600 \text{ mg/L}$; $m(\text{XWC}) = 1.3 \text{ g}$, $\text{pH}(\text{XWC}) = 12.0$; $m(\text{TAWC-1}) = 0.6 \text{ g}$, $\text{pH}(\text{TAWC-1}) = 8.0$; $m(\text{TAWC-2}) = 0.5 \text{ g}$; $\text{pH}(\text{TAWC-2}) = 8.0$; $m(\text{PAWC}) = 0.5 \text{ g}$; $\text{pH}(\text{PAWC}) = 8.0$; $m(\text{HAWC}) = 0.4 \text{ g}$; $\text{pH}(\text{PAWC}) = 7.0$.

out at room temperature. Weathered coal adsorption of Zn²⁺ occurs in two stages: the early stage during which adsorption is rapid (0–20 min) and the mid to late-stage during which adsorption is slow (25–80 min). The optimal reaction times of XWC, TAWC-1, TAWC-2, PAWC, and HAWC are 70, 30, 30, 25, and 25 min, respectively. In the early rapid stage, the concentration of Zn²⁺ at the interface of the weathered coal and wastewater is relatively high, resulting in substantial adsorption, and Zn²⁺ quickly occupies the adsorption sites on the outer surface of the pulverized coal. When Zn²⁺ enters the internal pores of pulverized coal, the interface $\rho(\text{Zn}^{2+})$ decreases, resulting in weaker adsorption kinetics and a decrease in removal rate.

3.2.4. Adsorption kinetics

In order to better explain the adsorption process of Zn²⁺ by weathered coal before and after modification, the adsorption processes at 25°C were fitted by pseudo-first-order and

pseudo-second-order kinetic equations, and their kinetic parameters were compared to determine the adsorption rate control procedure and adsorption mechanism during adsorption.

3.2.4.1. Pseudo-first-order kinetic model

The pseudo-first-order kinetic is generally the initial stage of the adsorption process, which is mainly monolayer adsorption by boundary diffusion and reflects the proportional relationship between the adsorption rate and the concentration of reactants. The pseudo-first-order kinetic model can be illustrated as follows [31]:

$$\frac{dQ_t}{dt} = k_1(Q_e - Q_t) \quad (3)$$

By integrating both sides of equation (3), the following equation can be obtained:

$$\log(Q_e - Q_t) = \log(Q_e) - k_1 t \quad (4)$$

where Q_e (mg/g) and Q_t (mg/g) are the adsorption capacities at equilibrium and at time t (min) respectively, and k_1 (min^{-1}) is a rate constant of first-order adsorption. The fitting results are shown in Fig. 8 and the parameters are shown in Table 3. For the five materials, the R^2 value of the pseudo-first-order kinetic model is not close to 1. Therefore, the

experimental data were further fitted with the second-order kinetic model.

3.2.4.2. Pseudo-second-order kinetic model

It is assumed that the adsorbent and adsorbent react chemically, and the adsorption rate is controlled by the mechanism of chemisorption. On this basis, a quasi-second-order adsorption kinetic model is established, in which electrons

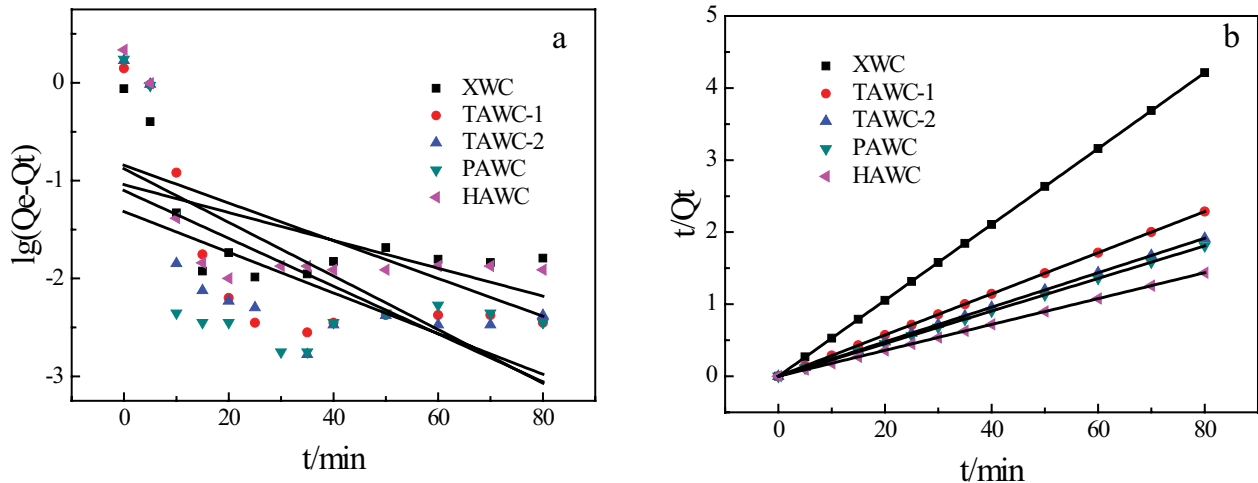


Fig. 8. Kinetic fitting curve of XWC, TAWC-1, TAWC-2, PAWC, and HAWC to Zn^{2+} adsorption. (a) Pseudo-first-order and (b) pseudo-second-order kinetic equations.

Table 3
Kinetic model parameters of XWC, TAWC-1, TAWC-2, PAWC, and HAWC adsorption of Zn^{2+}

Model type	Temperature	Adsorbent	Equation	Model constants	R^2
Pseudo-first-order kinetic equation	25	XWC	$y = -0.0142x - 1.0411$	$Q_e = 0.0327$ $k_1 = 0.0910$	0.3483
		TAWC-1	$y = -0.0274x - 0.8787$	$Q_e = 0.1322$ $k_1 = 0.0631$	0.5305
		TAWC-2	$y = -0.0244x - 1.1014$	$Q_e = 0.0792$ $k_1 = 0.0562$	0.4268
		PAWC	$y = -0.0208x - 1.1363$	$Q_e = 0.0731$ $k_1 = 0.0479$	0.2883
		HAWC	$y = -0.0193x - 0.8429$	$Q_e = 0.1436$ $k_1 = 0.0444$	0.3970
Pseudo-second-order kinetic equation	25	XWC	$y = 0.0526x + 0.0011$	$Q_e = 19.01$ $k_2 = 2.5156$	1
		TAWC-1	$y = 0.0286x + 0.0010$	$Q_e = 34.97$ $k_2 = 0.8177$	1
		TAWC-2	$y = 0.0239x + 0.0006$	$Q_e = 41.84$ $k_2 = 0.9520$	1
		PAWC	$y = 0.0226x + 0.0005$	$Q_e = 44.25$ $k_2 = 1.0215$	1
		HAWC	$y = 0.0180x + 0.0003$	$Q_e = 55.56$ $k_2 = 1.0800$	1

Note: Q_e is the equilibrium adsorption capacity (mg/g); k_1 is the pseudo-first-order kinetic model constant (min^{-1}); k_2 is the pseudo-second-order kinetic model constant ($\text{g}/(\text{mg min})$).

are gained and lost or shared. The pseudo-second-order kinetic model is described as [32]:

$$\frac{dQ_t}{dt} = k_2(Q_e - Q_t)^2 \quad (5)$$

By integrating both sides of Eq. (5), the following equation can be obtained:

$$\frac{t}{Q_t} = \left(\frac{1}{k_2 Q_e^2} \right) + \left(\frac{1}{Q_e} \right) t \quad (6)$$

where Q_e (mg/g) and Q_t (mg/g) are the adsorption capacities at equilibrium and at time t (min) respectively, and k_2 (min^{-1}) is a rate constant of second-order adsorption.

The fitting results are shown in Fig. 8 and the parameters are shown in Table 3. For the five materials, the R^2 value of the pseudo-second-order kinetic model is 1, which is higher than that of other kinetic models. The theoretical adsorption capacities of the four modified materials calculated by the pseudo-second-order kinetic model are 34.97, 41.84, 44.25, and 55.56 mg/g respectively, which is closer to the actual adsorption capacity. Therefore, the pseudo-second-order kinetic model more suitably describes the kinetics of the entire Zn^{2+} adsorption process. It shows that the adsorption process includes external liquid film diffusion, surface adsorption, and intraparticle diffusion. Chemical adsorption is the adsorption rate control step in the adsorption process [33].

3.2.5. Initial $\rho(\text{Zn}^{2+})$

The effects of different initial $\rho(\text{Zn}^{2+})$ on Zn^{2+} removal from wastewater by XWC, TAWC-1, TAWC-2, PAWC, and HAWC are shown in Fig. 9. The removal rates of Zn^{2+} by TAWC-1, TAWC-2, PAWC, and HAWC in the initial $\rho(\text{Zn}^{2+})$ range from 200 to 1,000 mg/L, stabilizes above 96%, and decrease with an increase in initial $\rho(\text{Zn}^{2+})$. With an initial $\rho(\text{Zn}^{2+}) > 600$ mg/L, the removal rate of Zn^{2+} by XWC decreases rapidly. Due to the limited adsorption sites per unit adsorbent, the increase of Zn^{2+} concentration increases the difference in ion concentration around the adsorption sites, promotes mass transfer, and the removal rate remains constant. With an increase in the amount of Zn^{2+} , the adsorption sites become gradually occupied to reach a state of saturation, resulting in a decrease in removal rate [34].

3.2.6. Isotherm models

In order to better describe the distribution of Zn^{2+} in the solution and adsorbent when the adsorption of Zn^{2+} by weathered coal before and after modification reaches equilibrium, the Langmuir and Freundlich isothermal adsorption models were used for linear fitting [35,36].

3.2.6.1. Freundlich isotherm

Freundlich adsorption isothermal equation is an empirical equation, which takes into account the energy heterogeneity of the adsorbent surface, and assumes that the

adsorption sites on the adsorbent surface are not evenly distributed and the energy of the adsorption sites is not the same. It describes the adsorption process as uneven multi-layer adsorption, and the particles interact after adsorption. Also applies to physical adsorption and chemical adsorption, but mainly the physical adsorption process. The mathematical expression of the Freundlich model can be written as [37]:

$$Q_e = kC^n \quad (7)$$

Eq. (7) can be linearized in logarithmic form, and the Freundlich constants can be determined as follows:

$$\log Q_e = \log K_f + n \log C_e \quad (8)$$

where K_f is the Freundlich constant related to adsorption capacity, n is the energy or intensity of adsorption, and C_e is the equilibrium concentration of Zn^{2+} (mg/L). The fitting results are shown in Fig. 10 and the parameters are shown in Table 4. The R^2 of the Freundlich isothermal adsorption model is not closer to 1.

3.2.6.2. Langmuir isotherm

Langmuir adsorption isotherm model is currently the most widely used adsorption isotherm model, applicable to physical adsorption and chemical adsorption types, and its equation is shown in Eq. (9) [38]:

$$\frac{C_e}{Q_e} = \frac{1}{Q_m b} + \frac{C_e}{Q_m} \quad (9)$$

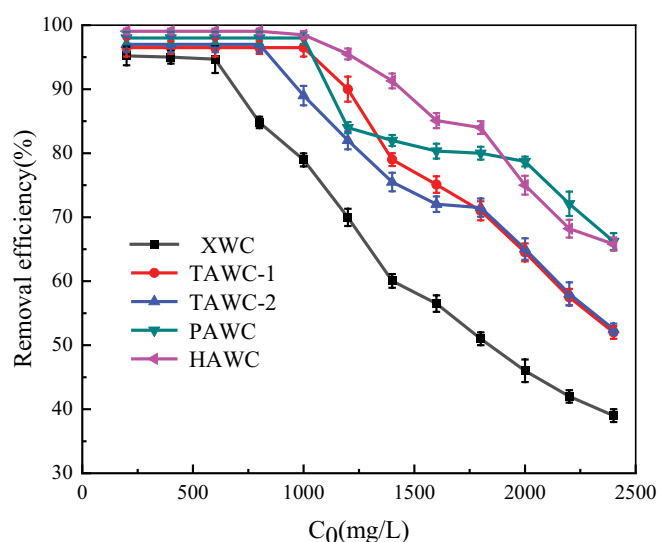


Fig. 9. Effects of initial concentration on Zn^{2+} removal. The adsorption temperature = 298 K; $m(\text{XWC}) = 1.3$ g; $\text{pH}(\text{XWC}) = 12.0$; $t(\text{XWC}) = 70$ min; $m(\text{TAWC-1}) = 0.6$ g; $\text{pH}(\text{TAWC-1}) = 8.0$; $t(\text{TAWC-1}) = 30$ min; $m(\text{TAWC-2}) = 0.5$ g; $\text{pH}(\text{TAWC-2}) = 8.0$; $t(\text{TAWC-2}) = 30$ min; $m(\text{PAWC}) = 0.5$ g; $\text{pH}(\text{PAWC}) = 8.0$; $t(\text{PAWC}) = 25$ min; $m(\text{HAWC}) = 0.4$ g; $\text{pH}(\text{PAWC}) = 7.0$; $t(\text{HAWC}) = 25$ min.

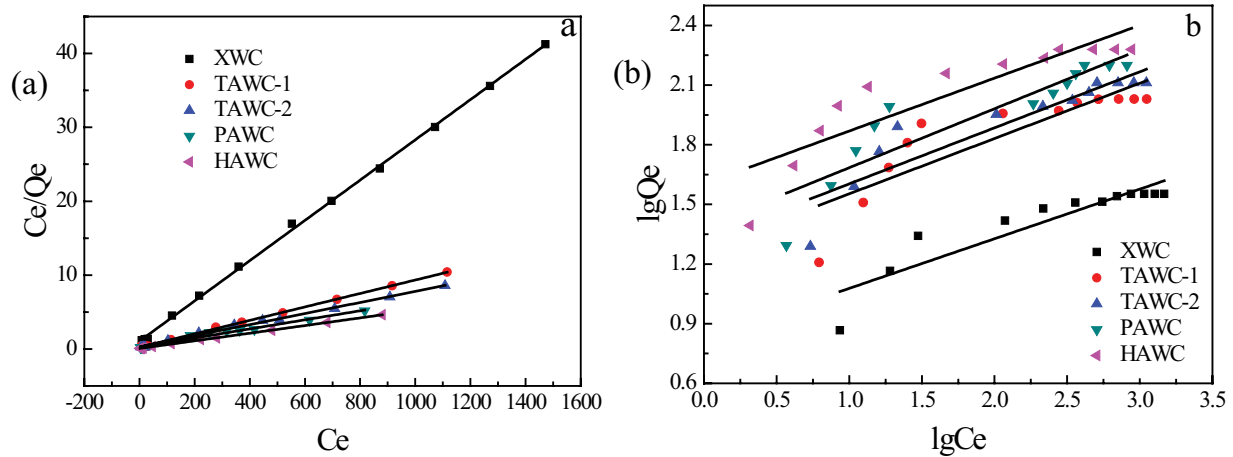


Fig. 10. Fitting curves of XWC, TAWC-1, TAWC-2, PAWC, and HAWC adsorption of Zn^{2+} : (a) Langmuir model and (b) Freundlich model.

Table 4
Adsorption isotherm model parameters of XWC, TAWC-1, TAWC-2, PAWC, and HAWC adsorption of Zn^{2+}

Model type	Adsorbent	Equation	Model constants	R^2
Langmuir isothermal adsorption model	XWC	$y = 0.0272x + 1.0612$	$Q_{max} = 36.76$ $K_L = 0.0256$	0.9993
	TAWC-1	$y = -0.0091x + 0.2337$	$Q_{max} = 109.89$ $K_L = 0.0389$	0.9994
	TAWC-2	$y = -0.0075x + 0.0359$	$Q_{max} = 133.23$ $K_L = 0.0245$	0.9955
	PAWC	$y = -0.0061x - 0.2556$	$Q_{max} = 163.93$ $K_L = 0.0239$	0.9808
	HAWC	$y = -0.0052x + 0.0679$	$Q_{max} = 192.31$ $K_L = 0.0766$	0.9995
Freundlich isothermal adsorption model	XWC	$y = 0.2496x + 0.8280$	$n = 4.0064$ $K_F = 6.7298$	0.8358
	TAWC-1	$y = 0.2782x + 1.2750$	$n = 3.5945$ $K_F = 18.8365$	0.7487
	TAWC-2	$y = 0.2819x + 1.3212$	$n = 3.5474$ $K_F = 20.9508$	0.8346
	PAWC	$y = 0.2965x + 1.3880$	$n = 3.3727$ $K_F = 24.4343$	0.8117
	HAWC	$y = 0.2659x + 1.6031$	$n = 3.7608$ $K_F = 40.0959$	0.7860

Note: Q_{max} is the monolayer saturated adsorption capacity of the adsorbent (mg/g); K_L is the equilibrium constant related to the affinity of the binding site (L/mg); n is the Freundlich constant representing the adsorption strength; K_F is the Freundlich constant representing the adsorption capacity of adsorbent $(L/mg)^{1/n}/(mg/g)$.

where Q_e is the amount adsorbed at equilibrium concentration C_e , Q_m is the Langmuir constant representing maximum monolayer adsorption capacity, and b is the Langmuir constant related to the energy of adsorption.

The R^2 of the Langmuir isothermal adsorption model is closer to 1, which better describes the adsorption of Zn^{2+} by XWC, TAWC-1, TAWC-2, PAWC, and HAWC (Fig. 10 and Table 4). The adsorption of Zn^{2+} by XWC, TAWC-1, TAWC-2, PAWC, and HAWC is predominantly monomolecular layer

adsorption and the lateral force among Zn^{2+} at different adsorption sites is zero. From the fitting calculation, the saturated adsorption capacity of XWC, TAWC-1, TAWC-2, PAWC, and HAWC is 36.76, 109.89, 133.23, 163.93, and 192.31 mg/g, respectively, and the saturated adsorption capacity of weathered coal after modification is 3.0, 3.6, 4.6, and 5.2 times higher than that before modification, respectively. Bashir et al. reported that the adsorption capacity of PSP biosorbent material for zinc ions in aqueous media

was 130.54 mg/g [39], Neethu et al. studied the adsorption capacity of PKM-2 from moringa oleic leaves for Zn (II) in aqueous solution, and its maximum adsorption capacity was 38.50 mg/g [40]. Ngabura et al. [41] investigated the adsorption of Zn (II) in simulated wastewater by hydrochloric acid-modified durian peel (HAMDP), with a maximum adsorption capacity of 36.73 mg/g. Compared with the above four sorbents, the four sorbents prepared in this experiment have better adsorption capacity for Zn²⁺, simple preparation, and low cost, they are better adsorbents.

4. Adsorption mechanism

In the kinetic data, the correlation coefficient R^2 of the pseudo-second-order kinetic model is closer to 1, and the fitting result of the equilibrium adsorption capacity is closer to the experimental value. Therefore, the pseudo-second-order kinetic model is more suitable to describe the whole kinetic process of Zn²⁺ adsorption, indicating that the adsorption process includes external liquid film diffusion, surface adsorption, intraparticle diffusion, etc. Chemisorption is the rate control step of the adsorption process, and the adsorption conforms to the Langmuir adsorption isotherm equation, indicating the adsorption of Zn²⁺ by the four sorbents is mainly monolayer adsorption, and the lateral force between Zn²⁺ at different adsorption sites is zero.

5. Conclusions

The adsorption of zinc by unmodified and modified weathered coal was analyzed and four adsorbents were compared by examining the influence of pH, amount of adsorbent, reaction time, and other factors on the adsorption process. The following conclusions were drawn:

- The characterization results show that the polyethyleneimine in the vinylamine was successfully grafted onto the surface of the pulverized coal after reaction with -C=O and -OH on the surface of the weathered coal. Moreover, with an increasing number of amino groups, the specific surface area, and pore volume showed a decreasing trend, while the aperture remained essentially unchanged.
- By examining the system pH, adsorbent dosage, initial $\rho(\text{Zn}^{2+})$, and other conditions, the four types of modified weathered coal were confirmed to have a removal rate over 96% in Zn²⁺-containing wastewater with concentrations $\leq 1,000$ mg/L under optimal adsorption conditions.
- The adsorption processes of Zn²⁺ by XWC, TAWC-1, TAWC-2, PAWC, and HAWC were consistent with the pseudo-second-order kinetic model and the Langmuir adsorption isotherm equation. The saturated adsorption capacities of XWC, TAWC-1, TAWC-2, PAWC, and HAWC were 36.76, 109.89, 133.23, 163.93, and 192.31 mg/g, respectively, which were 3.0, 3.6, 4.6 and 5.2 times higher than those before modification.

Acknowledgments

This study was funded by the General Project of Natural Science Foundation of Xinjiang Uygur Autonomous Region

(2020D01A75). We express our gratitude to the Physical and Chemical Testing Center of Xinjiang University for performing the scanning electron microscopy and the specific surface area, pore size, and XPS analysis.

References

- [1] C.K. Ahn, Y.M. Kim, S.H. Woo, J.M. Park, Removal of cadmium using acid-treated activated carbon in the presence of nonionic and/or anionic surfactants, *Hydrometallurgy*, 99 (2009) 209–213.
- [2] Y.G. Chen, R.Q. Huang, C.M. Zhu, D.B. Wu, Y.H. Sun, Y. He, W.M. Ye, Adsorptive removal of La(III) from aqueous solutions with 8-hydroxyquinoline immobilized GMZ bentonite, *J. Radioanal. Nucl. Chem.*, 299 (2014) 665–674.
- [3] A. Dabrowski, Z. Hubicki, P. Podkościelny, E. Robens, Selective removal of the heavy metal ions from waters and industrial wastewaters by ion-exchange method, *Chemosphere*, 56 (2004) 91–106.
- [4] B. Erdem, A. Özcan, A.S. Özcan, Adsorption and solid phase extraction of 8-hydroxyquinoline from aqueous solutions by using natural bentonite, *Appl. Surf. Sci.*, 256 (2010) 5422–5427.
- [5] F. Fu, Q. Wang, Removal of heavy metal ions from wastewaters: a review, *J. Environ. Manage.*, 92 (2011) 407–418.
- [6] D. Guaya, C. Valderrama, A. Farran, C. Armijos, J.L. Cortina, Simultaneous phosphate and ammonium removal from aqueous solution by a hydrated aluminum oxide modified natural zeolite, *Chem. Eng. J.*, 271 (2015) 204–213.
- [7] Y. Shio, H. Wataru, U. Kami, Study on specific heat of water adsorbed in zeolite using DSC, *Int. J. Thermophys.*, 31 (2010) 2004–2009.
- [8] M. Imbeault, M. Ouellet, M.J. Tremblay, Microarray study reveals that HIV-1 induces rapid type-I interferon-dependent p53 mRNA up-regulation in human primary CD4⁺ T cells, *Retrovirology*, 6 (2009) 1–14.
- [9] R. Li, M. Zhang, Y. Yang, Z.Q. Zhang, R. Qin, L. Wang, J.Z. Zheng, X.N. Sun, Adsorption of Pb(II) ions in aqueous solutions by common reed ash-derived SBA-15 modified by amino-silanes, *Desal. Water Treat.*, 55 (2015) 1554–1566.
- [10] M.L. Li, Z.Q. Zhang, R.H. Li, J.J. Wang, A. Ali, Removal of Pb(II) and Cd(II) ions from aqueous solution by thiosemicarbazide modified chitosan, *Int. J. Biol. Macromol.*, 86 (2016) 876–884.
- [11] K. Ma, L.Y. Cui, Y.Z. Dong, T.L. Wang, C. Da, G.J. Hirasaki, S.L. Biswal, Adsorption of cationic and anionic surfactants on natural and synthetic carbonate materials, *J. Colloid Interface Sci.*, 408 (2013) 164–172.
- [12] F. Martínez-Jerónimo, R. Villaseñor, G. Ríos, F. Espinosa-Chavez, Toxicity of the crude oil water-soluble fraction and kaolin-adsorbed crude oil on *Daphnia magna* (Crustacea: Anomopoda), *Arch. Environ. Contam. Toxicol.*, 48 (2005) 444–449.
- [13] M.M. Matlock, B.S. Howerton, M.A.V. Aelstyn, F.L. Nordstrom, D.A. Atwood, Advanced mercury removal from gold leachate solutions prior to gold and silver extraction: a field study from an active gold mine in Peru, *Environ. Sci. Technol.*, 36 (2002) 1636–1639.
- [14] S. Nethaji, A. Sivasamy, A.B. Mandal, Preparation and characterization of corn cob activated carbon coated with nano-sized magnetite particles for the removal of Cr(VI), *Bioresour. Technol.*, 134 (2013) 94–100.
- [15] D. Nibou, H. Mekatel, S. Amokrane, M. Barkat, M. Trari, Adsorption of Zn²⁺ ions onto NaA and NaX zeolites: kinetic, equilibrium and thermodynamic studies, *J. Hazard. Mater.*, 173 (2010) 637–646.
- [16] N.O. Omisanya, C.O. Folayan, S.Y. Aku, S.S. Adefila, R.B.O. Suleiman, Comparison of experimental measurements and simulation of solar (Zeolite4A-Water) adsorption refrigerator using Trnsys and Matlab Softwares, *Rev. Appl. Phys.*, 2 (2013) 114–127.
- [17] A.H. Oren, A. Kaya, Factors affecting adsorption characteristics of Zn²⁺ on two natural zeolites, *J. Hazard. Mater.*, 131 (2006) 59–65.
- [18] C.L. Peacock, D.M. Sherman, Surface complexation model for multisite adsorption of copper(II) onto kaolinite, *Geochim. Cosmochim. Acta*, 69 (2005) 3733–3745.

- [19] M. Rosu, A. Schumpe, Influence of surfactants on gas absorption into aqueous suspensions of activated carbon, *Chem. Eng. Sci.*, 62 (2007) 5458–5463.
- [20] P. Ganesan, R. Kamaraj, G. Sozhan, S. Vasudevan, Oxidized multiwalled carbon nanotubes as adsorbent for the removal of manganese from aqueous solution, *Environ. Sci. Pollut. Res.*, 20 (2013) 987–996.
- [21] R. Kamaraj, S. Vasudevan, Decontamination of selenate from aqueous solution by oxidized multi-walled carbon nanotubes, *Powder Technol.*, 274 (2015) 268–275.
- [22] M.B. Salzman, E.M. Smith, C. Koo, Excessive oral zinc supplementation, *J. Pediatr. Hematol. Oncol.*, 24 (2002) 582–584.
- [23] G.S. Simate, N. Maledi, A. Ochieng, S. Ndlovu, J. Zhang, L.F. Walubita, Coal-based adsorbents for water and wastewater treatment, *J. Environ. Chem. Eng.*, 4 (2016) 2291–2312.
- [24] P. Tan, J. Sun, Y.Y. Hu, Z. Fang, Q. Bi, Y.C. Chen, J.H. Cheng, Adsorption of Cu^{2+} , Cd^{2+} and Ni^{2+} from aqueous single metal solutions on graphene oxide membranes, *J. Hazard. Mater.*, 297 (2015) 251–260.
- [25] X.M. Tang, H.L. Zheng, H.K. Teng, Y.J. Sun, J.S. Guo, W.Y. Xie, Q.Q. Yang, W. Chen, Chemical coagulation process for the removal of heavy metals from water: a review, *Desal. Water Treat.*, 57 (2016) 1733–1748.
- [26] V.J. Vilar, C.M. Botelho, R.A. Boaventura, Equilibrium and kinetic modeling of Cd(II) biosorption by algae *Gelidium* and agar extraction algal waste, *Water Res.*, 40 (2006) 291–302.
- [27] M.E. Villanueva, A. Salinas, G.J. Copello, L.E. Díaz, Point of zero charge as a factor to control biofilm formation of *Pseudomonas aeruginosa*, in sol–gel derivatized aluminum alloy plates, *Surf. Coat. Technol.*, 254 (2014) 145–150.
- [28] J.F. Wu, Q.C. Xu, T. Bai, Adsorption behavior of some radionuclides on the Chinese weathered coal, *Appl. Radiat. Isot.*, 65 (2007) 901–909.
- [29] X. Ying, Z. Fang, Experimental research on heavy metal wastewater treatment with dipropyl dithiophosphate, *J. Hazard. Mater.*, 137 (2006) 1636–1642.
- [30] X.Z. Yuan, Y.T. Meng, G.M. Zeng, Y.Y. Fang, J.G. Shi, Evaluation of tea-derived biosurfactant on removing heavy metal ions from dilute wastewater by ion flotation, *Colloids Surf., A*, 317 (2008) 256–261.
- [31] R. Kamaraj, S. Vasudevan, Facile one-pot synthesis of nano-zinc hydroxide by electro-dissolution of zinc as a sacrificial anode and the application for adsorption of Th^{4+} , U^{4+} , and Ce^{4+} from aqueous solution, *Res. Chem. Intermed.*, 42 (2016) 4077–4095.
- [32] R. Kamaraj, A. Pandiarajan, M.R. Gandhi, A. Shibayama, S. Vasudevan, Eco-friendly and easily prepared graphene nanosheets for safe drinking water: removal of chlorophenoxycetic acid herbicides, *ChemistrySelect*, 2 (2017) 342–355.
- [33] G.M. Zeng, Y.Y. Liu, T. Lin, G.D. Yang, Y. Pang, Y. Zhang, Enhancement of Cd(II) adsorption by polyacrylic acid modified magnetic mesoporous carbon, *Chem. Eng. J.*, 259 (2015) 153–160.
- [34] J. Zhang, Y.Q. Wu, J.L. Wang, Y.P. Wang, Y.P. Wang, Improved properties of weathered coal and SBR/weathered coal compound modified asphalt, *Iran. Polym. J.*, 16 (2007) 251–259.
- [35] J. Zhang, J.L. Wang, Y.Q. Wu, Y.P. Wang, Y.P. Wang, Evaluation of the improved properties of SBR/weathered coal modified bitumen containing carbon black, *Constr. Build. Mater.*, 23 (2009) 2678–2687.
- [36] S.Q. Zhang, L. Yuan, W. Li, Z. Lin, Y.T. Li, S.W. Hu, B.Q. Zhao, Characterization of pH-fractionated humic acids derived from Chinese weathered coal, *Chemosphere*, 166 (2017) 334–342.
- [37] S. Vasudevan, J. Lakshmi, G. Sozhan, Optimization of the process parameters for the removal of phosphate from drinking water by electrocoagulation, *Desal. Water Treat.*, 12 (2009) 407–414.
- [38] S.V. Lakshmi, Process conditions and kinetics for the removal of copper from water by electrocoagulation, *Environ. Eng. Sci.*, 29 (2012) 563–572.
- [39] A. Bashir, T. Manzoor, L.A. Malik, Enhanced and selective adsorption of Zn(II), Pb(II), Cd(II), and Hg(II) ions by a dumbbell- and flower-shaped potato starch phosphate polymer: a combined experimental and DFT calculation study, *ACS Omega*, 5 (2020) 4853–4867.
- [40] J. Neethu, B.M.L. Deepak, A.S. Thalikkassery, Central composite design for adsorption of Pb(II) and Zn(II) metals on PKM-2 *Moringa oleifera* leaves, *ACS Omega*, 6 (2021) 25277–25298.
- [41] M. Ngabura, S.A. Hussain, W. Ghani, M.S. Jami, Y.P. Tan, Utilization of renewable durian peels for biosorption of zinc from wastewater, *J. Environ. Chem. Eng.*, 6 (2018) 2528–2539.